Performance of a Coded Non-Square Quadrature Amplitude Modulation Scheme over Fading Channels

L. Li,[1] D. Divsalar,[1] and S. Dolinar[1]

It is shown that a non-square (NS) 2^{2n+1}-ary quadrature amplitude modulation (QAM) can be decomposed into a single-parity-check (SPC) block encoder and a memoryless modulator with independent in-phase (I) and quadrature (Q) symbol mapping. When NS-2^{2n+1}-QAM is concatenated with a forward-error-correcting (FEC) code, iterative demodulation and decoding of the FEC code and the inherent SPC code of NS-2^{2n+1}-QAM exploits the modulation's inherent memory and its independent I- and Q-channel mapping and demapping. The capacity and the bit-/symbol-error-rate (BER/SER) performance of coded and uncoded NS-2^{2n+1}-QAM systems are given for both additive white Gaussian noise (AWGN) channels and Rayleigh fading channels and are compared to those of other conventional 2^{2n+1}-ary systems. Simulation results show that, with iterative demodulation and decoding, coded NS-8QAM outperforms three conventional 8-ary systems by at least 0.65 dB on AWGN channels and by at least 0.57 dB on Rayleigh fading channels at BER $= 10^{-5}$, when the FEC code is a concatenation of (15,11) Hamming codes with rate-1 accumulator codes, while coded NS-32QAM outperforms standard 32QAM by about 0.45 dB on AWGN channels and by about 0.27 dB on Rayleigh fading channels.

I. Introduction

Shortly after the introduction of the revolutionary turbo codes consisting of parallel concatenated convolutional codes (PCCC) in 1993 [1], serially concatenated codes (SCC) were shown to have comparable performance [2,3]. Since then it has been realized that some modulation schemes have inherent memory, which could be made explicit and serve as an inner code in a coded system with iterative decoding. Such modulation schemes include continuous phase modulation (CPM)[4–7], differential phase shift keying (DPSK), and differential quaternary phase shift keying (DQPSK) [8–11]. It was shown that the inherent recursive convolutional code of these modulation schemes combined with an interleaver significantly improves the distance spectrum of the transmitted signals and therefore yields large coding gains [10]. Two other modulation schemes that have memory are Feher-patented QPSK (FQPSK) [12] and military

[1] Communications Systems and Research Section.

The research described in this publication was carried out by the Jet Propulsion Laboratory, California Institute of Technology, under a contract with the National Aeronautics and Space Administration.

standard shaped offset QPSK (MIL-STD SOQPSK).[2] By using a representation of FQPSK and MIL-STD SOQPSK as trellis-coded modulations, large coding gains are achievable even when simple outer codes are used [13–15].[3]

In applications that require high bandwidth efficiency, high-order modulation schemes such as M-ary quadrature amplitude modulation (QAM) ($M > 4$) are often considered. In this article, we will show that a non-square (NS) 2^{2n+1}-QAM ($n = 1, 2, \cdots$) also has inherent memory. In other words, NS-2^{2n+1}-QAM is by itself a form of coded modulation. Specifically, we will show that NS-2^{2n+1}-QAM can be decomposed into a $(2n + 2, 2n + 1)$ single-parity-check (SPC) encoder and a memoryless modulator, where an independent in-phase (I) and quadrature (Q) signal mapping is possible. Figure 1 gives the block diagram of a coded system with NS-2^{2n+1}-QAM modulation. In this figure, input data are first encoded by a forward-error-correcting (FEC) encoder. The encoded bits then are permuted by a random interleaver π before every $2n + 1$ bits are mapped into an NS-2^{2n+1}-QAM symbol. It will be shown in Section II that the mapping process is equivalent to the following. First, the $2n + 1$ bits are passed through a $(2n + 2, 2n + 1)$ SPC encoder. Then the $2n + 2$ output bits are evenly divided into two groups. Each group of $n + 1$ output bits is mapped to a 2^{n+1}-ary pulse amplitude modulation (PAM) symbol. Then the two 2^{n+1}-PAM symbols are transmitted through the I and Q channels independently.

We will show that this decomposition of NS-2^{2n+1}-QAM can be applied to obtain joint iterative demodulation and decoding algorithms in a coded system that exploit the inherent memory of NS-2^{2n+1}-QAM and achieve better coding gains. In addition, the decoding complexity can be reduced to that of 2^{n+1}-PAM systems. In practice, we will see that NS-2^{2n+1}-QAM can be implemented by using existing 2^{2n+2}-QAM hardware directly, since its signal constellation is just a subset of the 2^{2n+2}-QAM square constellation. We then will compare the capacity and bit-/symbol-error-rate (BER/SER) performances of coded and uncoded NS-2^{2n+1}-QAM systems with those of other 2^{2n+1}-ary modulation schemes on both additive white Gaussian noise (AWGN) and Rayleigh fading channels.

The remainder of the article is organized as follows. In Section II, we show the decomposition of NS-2^{2n+1}-QAM and the recursive convolutional nature of its inherent SPC code. We describe the iterative demodulation and decoding of coded NS-2^{2n+1}-QAM systems in Section III, using as an example a novel serially concatenated code composed of (15,11) Hamming outer codes and rate-1 accumulator inner codes. The capacity and uncoded system performance comparisons of NS-2^{2n+1}-QAM and other 2^{2n+1}-ary schemes are given in Section IV for both AWGN and Rayleigh fading channels. In Section V, we present simulation results of coded NS-2^{2n+1}-QAM system performances on both AWGN and Rayleigh fading channels and compare them to those of other 2^{2n+1}-ary systems. Finally, our conclusions are given in Section VI.

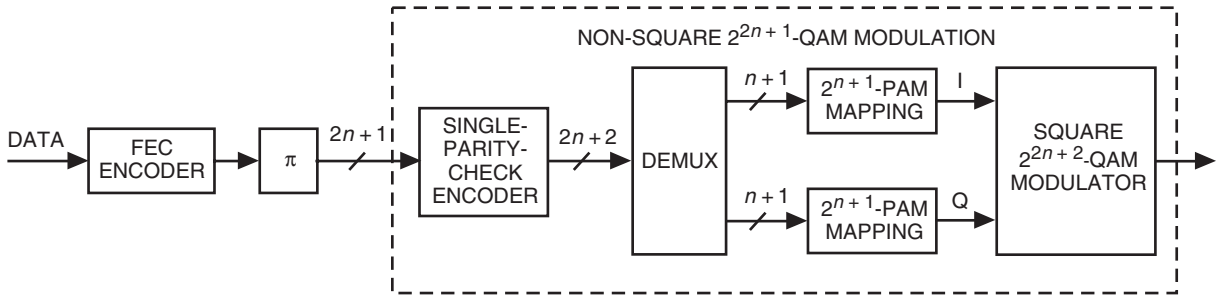

Fig. 1. A coded system with NS-2^{2n+1}-QAM modulation.

[2] L. Li and M. K. Simon, "Performance of Coded OQPSK and MIL-STD SOQPSK with Iterative Decoding," submitted for publication to *IEEE Transactions on Communication*.

[3] Ibid.

II. Decomposition of NS-2^{2n+1}-QAM

We study the NS-2^{2n+1}-QAM constellation as proposed in [17]. To obtain this NS-2^{2n+1}-QAM constellation, we start with the square constellation for 2^{2n+2}-QAM with independent I-dimension and Q-dimension Gray-code (GC) mapping.[4] That is, each dimension of the square 2^{2n+2}-QAM is an independent 2^{n+1}-PAM with GC mapping. There are 2^{2n+2} signal points in the square 2^{2n+2}-QAM constellation. The GC label of each signal point can be obtained easily by concatenating its I-dimension GC label with its Q-dimension GC label. Now by deleting every other point in each dimension, we have only half of the points left in each row and half of the points left in each column. The remaining points in each row have the same distance between them, and so do the remaining points in each column. The total number of remaining points is 2^{2n+1}, and these points form the non-square constellation for NS-2^{2n+1}-QAM. Figures 2 and 3 show the resulting non-square constellations of NS-8QAM ($n = 1$) and NS-32QAM ($n = 2$), respectively.

Now instead of re-labeling the 2^{2n+1} points as shown in [17], we keep their labels unchanged. That is, the labels for these remaining 2^{2n+1} points are the same as in the square 2^{2n+2}-QAM constellation. This means that $2n + 2$ bits are used to label each of the 2^{2n+1} points in the NS-2^{2n+1}-QAM constellation: $n+1$ bits (denoted as $I_1, \cdots, I_{n+1}$) for the I-dimension labeling, and $n+1$ bits (denoted as $Q_1, \cdots, Q_{n+1}$) for the Q-dimension labeling. However, we know that each point in a 2^{2n+1}-QAM constellation represents only $2n + 1$ bits of information. Therefore, the $2n + 2$ bits used for labeling an NS-2^{2n+1}-QAM signal point are not independent. Close examination shows that, for any signal point in the NS-2^{2n+1}-QAM constellation, the last bit of its $2n+2$ labeling bits can be viewed as a parity-check bit of the other $2n+1$ bits. In other words, if we label an NS-2^{2n+1}-QAM signal point as $I_1 \cdots I_{n+1} Q_1 \cdots Q_{n+1}$, then

$$Q_{n+1} = \left(\sum_{i=1}^{n+1} I_i + \sum_{i=1}^{n} Q_i \right) \mod 2 \tag{1}$$

For example, when $n = 1$ and an NS-8QAM signal point is labeled as $I_1 I_2 Q_1 Q_2$, then $Q_2 = I_1 \oplus I_2 \oplus Q_1$, where $\oplus$ denotes "exclusive OR" operation. This can be easily verified for symbol labels shown in Fig. 2.

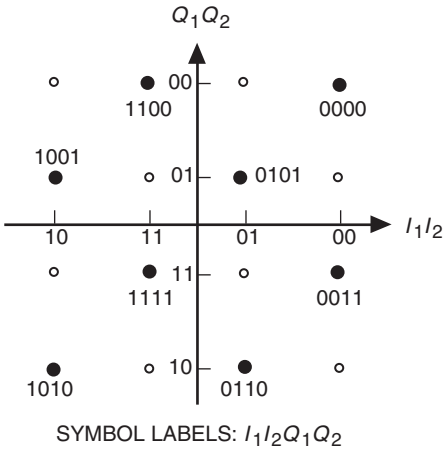

Fig. 2. NS-8QAM signal constellation.

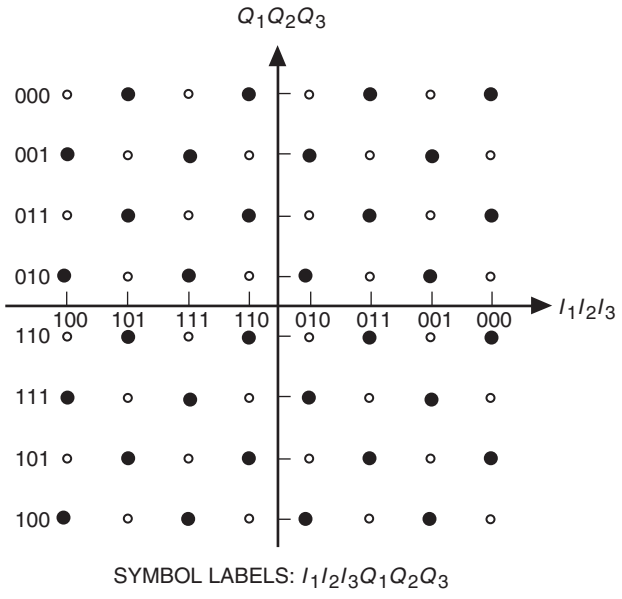

Fig. 3. NS-32QAM signal constellation.

[4] Other kinds of mappings also are applicable if desired.

Therefore, each NS-2^{2n+1}-QAM symbol can be generated by first encoding the corresponding $2n+1$ bits with a $(2n+2, 2n+1)$ SPC block encoder and then using the $2n+2$ encoded bits to select one of the $2n+1$ points on the NS-2^{2n+1}-QAM constellation. Specifically, the I-dimensional position and the Q-dimensional position of a signal point on an NS-2^{2n+1}-QAM constellation can be independently determined by the first $n+1$ encoded bits and the remaining $n+1$ encoded bits, respectively.

Similar to the convolutional encoding of the (n, k) Hamming code in [16], the $(2n+2, 2n+1)$ SPC block code can be generated as a recursive, systematic, terminated convolutional code with two states. The convolutional encoder structure of this SPC code is shown in Fig. 4. For the first input $2n+1$ bits, the switch in Fig. 4 is connected to point A, and the $2n+1$ input bits at point A will emerge as the first $2n+1$ encoded bits. After the $2n+1$ bits, the switch in Fig. 4 is toggled to point B to produce an additional encoded bit. This additional bit will be the same as the feedback bit, which is the parity-check bit for the previous $2n+1$ bits.

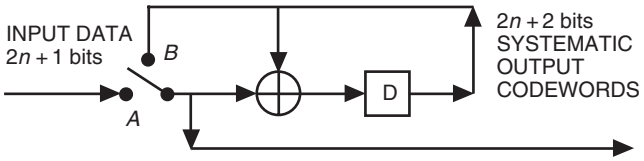

Fig. 4. A recursive convolutional structure for a $(2n+2, 2n+1)$ SPC encoder.

Although it is easily seen that each signal point on the NS-2^{2n+1}-QAM constellation can be uniquely determined and labeled with the $2n+1$ input bits only (i.e., without the parity-check bit Q_{n+1}), there are two obvious advantages for the decomposition of the NS-2^{2n+1}-QAM into a recursive convolutional encoder and a memoryless modulator with independent I-dimension and Q-dimension GC mapping. First, when NS-2^{2n+1}-QAM is used in a coded system, the decomposition can be applied to obtain iterative demodulation and decoding algorithms so as to achieve better coding gains.[5] The second obvious advantage is that, when performing iterative demodulation and decoding, the computational complexity for determining the log-likelihood ratio (LLR) of each bit is reduced dramatically due to the independent I-dimension and Q-dimension mapping/demapping of the NS-2^{2n+1}-QAM signals. In particular, for a coded M-ary modulation system, if independent I and Q mapping and demapping are not possible, computing the LLR for each bit of a signal point with a received symbol requires calculation of the distance between the received symbol and each of the M points on the M-ary signal constellation. That is, M distinct Euclidian distances have to be calculated and compared for each bit with a given received symbol. However, in the case of independent I and Q mapping/demapping, since each bit of a signal point is involved in only one-dimensional mapping/demapping, computing its LLR with a received symbol is now equivalent to that of a one-dimensional modulation system. For example, since the NS-2^{2n+1}-QAM signal mapping can be decomposed into two independent 2^{n+1}-PAM mappings (one in each dimension), computing the LLR for each bit requires calculating only 2^{n+1} Euclidian distances in a single dimension instead of 2^{2n+1} distances in two dimensions. More details about the iterative demodulation and decoding procedure will be given in Section III.

III. Iterative Demodulation and Decoding

We now consider the case where the FEC scheme in Fig. 1 is a serial concatenation of high-rate (15,11) Hamming outer codes and simple two-state, rate-1 accumulator inner codes, separated by a novel "parallel interleaver" that allows decoding with a parallel architecture at very high speeds, on the order

[5] We have shown in L. Li, D. Divsalar, and S. Dolinar, "Iterative Demodulation, Demapping, and Decoding of Coded Non-Square QAM," submitted for publication to *IEEE Transactions on Communication*, that iterative demapping can be applied to coded NS-2^{2n+1}-QAM at the same time to achieve further coding gains at the expense of increased complexity.

of 1 gigabit per second (Gbps) [16]. When combined with NS-2^{2n+1}-QAM, it can achieve a bandwidth efficiency of $(2n+1) \times 11/15$ bits/s/Hz (or bps/Hz).

The encoder structure of this concatenated code is shown in Fig. 5. In this figure, there are 372 parallel Hamming encoders and 15 parallel accumulating encoders. The block interleaver in the middle has 372 rows and 15 columns. There is a random interleaver π of size 15 following each Hamming encoder. It permutes the 15 output bits of the Hamming encoder before they are written into the corresponding row of the block interleaver. Each of the 372 random interleavers has a distinct permutation pattern. The data in the block interleaver are read out column by column. Before the data in each column are encoded by an accumulating encoder, they are permuted by an S-random interleaver π of size 372. There are 15 such S-random interleavers, and each of them also has a distinct permutation pattern. This encoder structure yields an overall code of length 5580 (15×372) and dimension 4092 (i.e., there are 11×372 input bits).

In this figure, we indicate that a desired input data rate of 1.116 Gbps can be obtained by running the 372 Hamming encoders at 3 Mbps each, and the 15 accumulating encoders at 101 Mbps each. The outputs of the 15 accumulating encoders are mapped into NS-2^{2n+1}-QAM signal points. With NS-8QAM, the first output bits of the first three accumulators are used to choose one of the 8 signal points on the non-square constellation as shown in Fig. 2. Then the first output bits of the next three accumulators are used to choose the second NS-8QAM symbol and so on, until the first five NS-8QAM symbols are produced. Then the next five NS-8QAM symbols are created using the second bits from three accumulators at a time, and so forth. With NS-32QAM, we take output bits five at a time from five separate accumulators to form each NS-32QAM symbol, stepping through the 15 accumulator codes in a cyclic order until all 5580 output bits are mapped. This type of mapping eliminates the need for a channel interleaver.

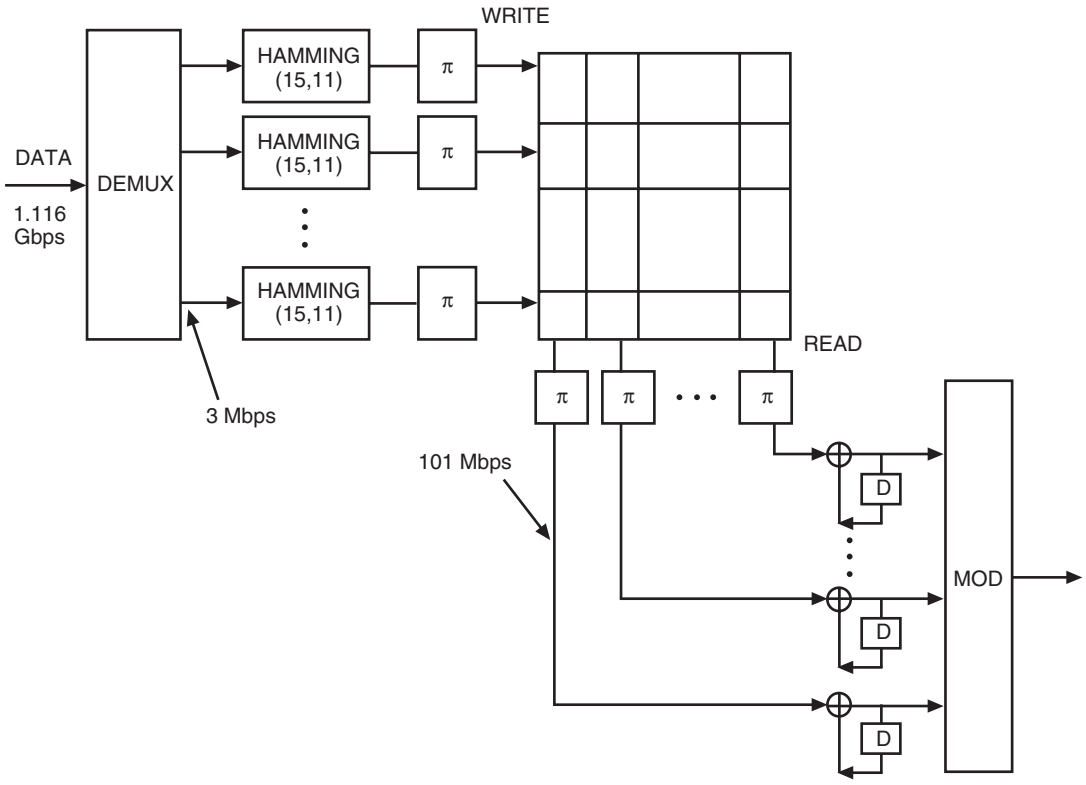

Fig. 5. Encoder structure for the Hamming and accumulator code.

We now show how to perform iterative demodulation and decoding when this serially concatenated Hamming and accumulator code is combined with the proposed NS-2^{2n+1}-QAM to achieve good power and bandwidth efficiency at a very high decoding rate. There are two different methods to decode the three constituent codes (i.e., the inherent SPC code of NS-2^{2n+1}-QAM, the accumulator code, and the Hamming code). One method involves separate decoding of the accumulator code and the SPC code, while the other performs joint decoding of the two codes.

A. Separate Decoding of Accumulator Codes and SPC Codes

Figure 6 shows the decoder structure for decoding the three serially concatenated codes separately. Note that each of the three constituent codes has a time-invariant trellis representation due to its recursive convolutional structure. The soft-input soft-output (SISO) module [18,19] applying the Bahl–Cocke–Jelinek–Raviv (BCJR) algorithm [20] on a time-invariant trellis is used to decode each constituent code.

Specifically, in this figure, given the received I- and Q-channel observations for each symbol, the reliabilities (or LLRs) for the $n+1$ bits (i.e., $I_1, \cdots, I_{n+1}$) assigned to I-dimension labels of an NS-2^{2n+1}-QAM symbol are calculated based on the I-channel observations only, and the reliabilities for the other $n+1$ bits (i.e., $Q_1, \cdots, Q_{n+1}$) assigned to Q-dimension labels are calculated based on the Q-channel observations only. The observation-based reliabilities for all $2n+2$ bits (i.e., $I_1, \cdots, I_{n+1}, Q_1, \cdots, Q_{n+1}$) provided by the I and Q demappers as well as the properly demultiplexed extrinsic information for all bits but Q_{n+1} from the accumulator SISO modules are used in the SISO module for the SPC code. For the $(2n+2, 2n+1)$ systematic SPC code, the first $2n+1$ bits (i.e., $I_1, \cdots, I_{n+1}, Q_1, \cdots, Q_n$) are just information bits, which means they are direct output bits of the accumulators. Therefore, after being properly multiplexed and demultiplexed, the observation-based reliabilities for these $2n+1$ bits will be used directly in the SISO modules for the accumulator codes. In addition, there is still extrinsic information from the SISO module of the SPC code for these $2n+1$ bits. In this case, care must be taken when calculating such extrinsic information. In particular, for the length $2n+2$ SPC code, the extrinsic

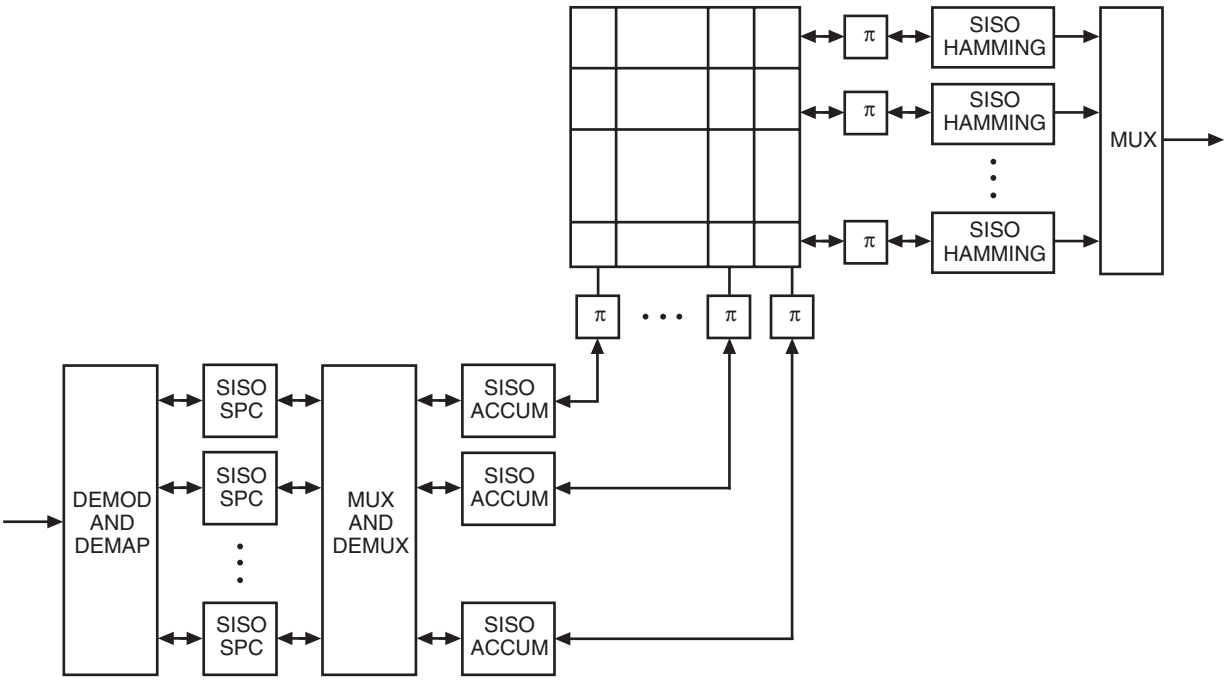

Fig. 6. Decoder structure for separate decoding of the inherent SPC code and the Hamming and accumulator code.

information for each of its first $2n+1$ bits should now be derived from all observation-based reliabilities except that of itself, instead of from all $2n+2$ reliabilities including that of itself. Details on the essential information exchange between SISO modules for serially concatenated convolutional codes are clarified in [21].

B. Joint Decoding of Accumulator Codes and SPC Codes

Since there is no interleaver between the accumulator codes and the inherent SPC codes of NS-2^{2n+1}-QAM as shown in Fig. 5, we can view the concatenation of $2n+1$ accumulator codes and a $(2n+2, 2n+1)$ SPC code as a single joint code with $2n+2$ output bits for every $2n+1$ input bits. The structure of this joint code is shown in Fig. 7. By using a single SISO module for this joint code instead of one SISO module for the SPC code and one SISO module for each of the $2n+1$ accumulator codes as illustrated in Fig. 6, we expect to achieve better coding gains. This is verified by our simulation results in Section V. However, the decoding complexity of this single SISO module using the joint trellis of the $2n+1$ accumulator codes and the $(2n+2, 2n+1)$ SPC code is much greater than that of separate SISO modules for decoding the SPC code and each of the $2n+1$ accumulator codes.

IV. Capacity and Uncoded System Performance Comparison

In this section, we compare the capacity of the proposed NS-2^{2n+1}-QAM ($n = 1, 2$) on both AWGN and Rayleigh fading channels to that of other 2^{2n+1}-ary signal constellations. We also compare the SER of uncoded NS-2^{2n+1}-QAM ($n = 1, 2$) systems to that of other 2^{2n+1}-ary systems on both kinds of channels. For NS-32QAM, we compare its performance to that of standard 32QAM, the constellation of which has the "central-square-with-four-wings" structure [22]. For NS-8QAM, we compare its performance to that of standard 8QAM, star-8QAM, and 8PSK. Figure 8 shows the constellations for standard 8QAM and star-8QAM. In [23], star-8QAM was considered to be the best 8QAM since it offers the largest "squared minimum distance to average power" ratio.

Comparing Figs. 2 and 8(a), we note that, although labeled differently, the standard 8QAM constellation is essentially the same as that of NS-8QAM, if we rotate it counter-clockwise by 45 deg. Therefore, these two 8QAM schemes will have the same capacity and the same SER in an uncoded system.

A. Symbol-Error Rate

1. AWGN Channel. Since it is hard to derive the exact SER for these modulation schemes, for comparison purposes we compute approximate upper bounds. For a given signal constellation, assuming maximum-likelihood detection and large signal-to-noise ratio (SNR), an approximate upper bound for the SER P_e on an AWGN channel can be expressed as [24]

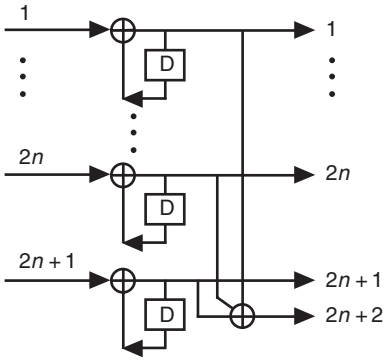

Fig. 7. Code structure of the joint accumulator codes and the SPC code.

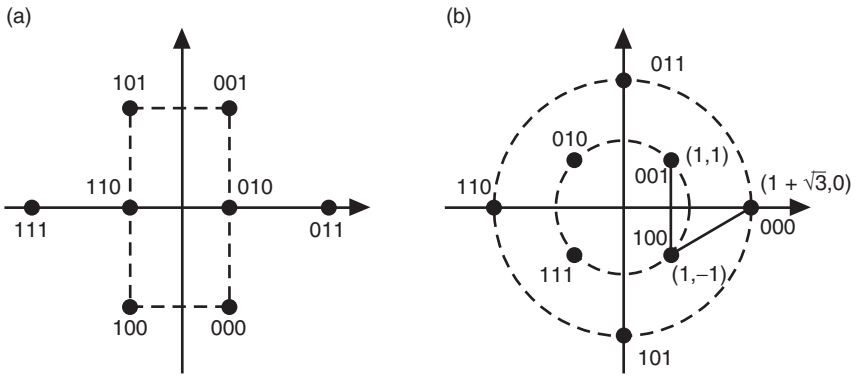

Fig. 8. Signal constellations for (a) standard 8QAM and (b) star-8QAM.

$$P_e \leq c_1 \cdot \ \text{erfc}\left(\sqrt{c_2 \frac{E_b}{N_0}}\right) \tag{2}$$

where c_1 and c_2 are constants determined by the constellation, erfc$(\cdot)$ is the complementary error function, and E_b/N_0 is the SNR per bit. The constant c_2 is proportional to the constellation's ratio of squared minimum distance to average power. For star-8QAM, $c_1 = 3/2$ and $c_2 = (3-\sqrt{3})/2 \simeq 0.634$; for both standard 8QAM and NS-8QAM, $c_1 = 9/8$ and $c_2 = 3/5 = 0.6$; for 8PSK, $c_1 = 1$ and $c_2 = 3\sin^2(\pi/8) \simeq 0.439$; for standard 32QAM, $c_1 = 13/8$ and $c_2 = 3/20 = 0.15$; and for NS-32QAM, $c_1 = 49/32$ and $c_2 = 3/21 \simeq 0.143$.

Figure 9 shows this upper bound for each of the six modulation schemes. From this figure, we see that, for large E_b/N_0, star-8QAM does perform slightly better than NS-8QAM and standard 8QAM. In addition, all three 8QAM schemes have much better SER than 8PSK, as expected. Among 32-ary modulations, standard 32QAM performs slightly better than NS-32QAM.

2. Rayleigh Fading Channel. The approximate SER upper bounds for the six modulation schemes in the presence of Rayleigh fading can be obtained easily by averaging the instantaneous E_b/N_0 in the right-hand side of Eq. (2) over the Rayleigh probability density function of E_b/N_0 in fading. By following the method described in [25], we have

$$P_e \leq c_1 \cdot \left(1 - \sqrt{\frac{c_2 \cdot E_b/N_0}{1 + c_2 \cdot E_b/N_0}}\right) \tag{3}$$

where c_1 and c_2 are the same constants used in Eq. (2).

Figure 10 shows this upper bound for each of the six modulation schemes. From this figure, we see that, unlike the case of AWGN channels, star-8QAM has the worst performance in Rayleigh fading and 8PSK has very similar performance to that of star-8QAM. For large E_b/N_0, NS-8QAM and standard 8QAM perform nearly 1 dB better than star-8QAM and 8PSK. Among 32-ary modulations, the performances of NS-32QAM and standard 32QAM are virtually indistinguishable.

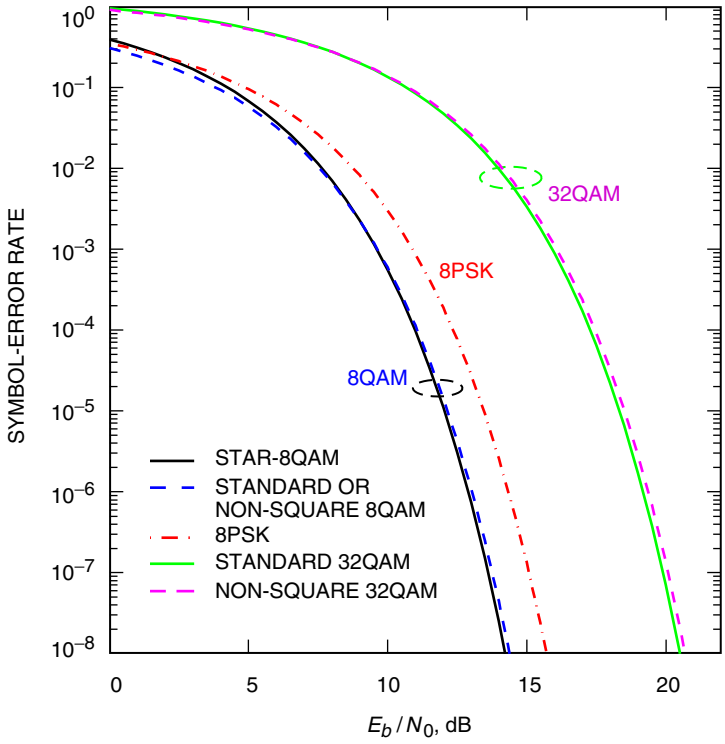

Fig. 9. SER upper bounds for the six uncoded modulation schemes on an AWGN channel.

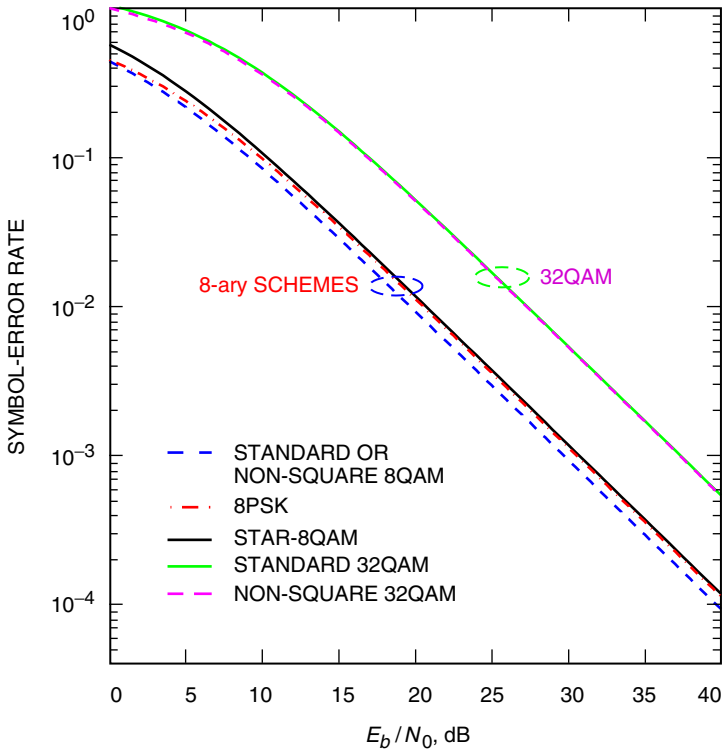

Fig. 10. SER upper bounds for the six uncoded modulation schemes on a Rayleigh fading channel.

B. Capacity on AWGN and Rayleigh Fading Channels

We use the method described in [26] to calculate the capacity or bandwidth efficiency in bps/Hz for the six different modulation schemes on an AWGN channel. The capacity of each modulation scheme in Rayleigh fading is obtained by averaging the instantaneous E_b/N_0 in the capacity formula for AWGN channels over a Rayleigh distribution. Figures 11 and 12 show the numerical results for AWGN and Rayleigh fading channels, respectively. In both figures, we see that all three 8QAM schemes have obviously larger capacity than 8PSK. However, the capacity of NS-8QAM and standard 8QAM is slightly larger than that of star-8QAM, although uncoded star-8QAM has better SER performance at high E_b/N_0 on AWGN channels, as shown in Fig. 9. For 32-ary modulations, standard 32QAM yields a slightly higher capacity than NS-32QAM, but the difference is negligible.

V. Coded System Performance Comparison

In this section, we show simulation results for the six modulation schemes used in a coded system on both AWGN and Rayleigh fading channels. The FEC code in each case is the concatenation of (15,11) Hamming codes with rate-1 accumulator codes described in Section III. For NS-8QAM and NS-32QAM, the iterative demodulation and decoding procedure with either separate or joint decoding of the accumulator codes and the SPC codes as described in Section III is applied. For the other three 8-ary systems (i.e., standard 8QAM, star-8QAM, and 8PSK) and for standard 32QAM, iterative decoding of the Hamming codes and of the accumulator codes using the standard BCJR algorithm is performed after demodulation.

Since GC labeling is impossible for 2^{2n+1}-QAM ($\forall n \geq 1$) [22], in our simulations we have adopted a quasi-GC labeling for standard 8QAM as shown in Fig. 8. Figure 8 also shows the labels used in our simulations for star-8QAM, which are similar to the GC labels used in our simulations for 8PSK. The quasi-GC labeling for standard 32QAM is adopted from the labeling scheme demonstrated in "Case 1" of Fig. 15 in [22]. For each 8-ary modulation, the overall bandwidth efficiency (throughput) of the coded system using the (15,11) Hamming codes and the accumulator codes is 2.2 bps/Hz. For each 32-ary modulation, the overall bandwidth efficiency of the coded system is 3.67 bps/Hz. BER results are given in the next two subsections for each of the 6 coded modulation systems.

A. AWGN Channel

Figure 13 compares the BER performance of the four 8-ary coded modulation systems on an AWGN channel. We see that coded NS-8QAM, with iterative demodulation and joint decoding of the accumulator codes and the SPC code, requires an E_b/N_0 of 4.2 dB to achieve BER $= 10^{-5}$ with 10 iterations. This is about 1.33 dB from the capacity limit of 2.87 dB for NS-8QAM as shown in Fig. 11 at the coded modulation system's throughput of 2.2 bps/Hz. At this BER and number of iterations, NS-8QAM outperforms standard 8QAM by 0.65 dB despite having the same capacity limit. There is a small loss of about 0.15 dB for NS-8QAM when the simpler, separate decoding of the accumulator codes and the SPC code is substituted for joint decoding.

Figure 13 also shows the surprising fact that coded star-8QAM performs only about as well as 8PSK at BER $= 10^{-5}$, despite having a 0.43 dB capacity advantage over 8PSK at a throughput of 2.2 bps/Hz. Indeed, as shown in Fig. 9, uncoded star-8QAM is about 1.6 dB better than uncoded 8PSK and about 0.24 dB better than 8QAM and NS-8QAM asymptotically. However, the coded system with star-8QAM performs about 0.2 dB worse than the one with standard 8QAM, and much worse than the coded system with NS-8QAM. The reason that coded star-8QAM with iterative decoding does not perform well may be due to the fact that each of the four points on the inner circle of its constellation has four adjacent points with minimum distance, which makes it hard to come up with a good labeling system. Simulation results in Fig. 13 imply that the star-8QAM labels in Fig. 8 are probably not good enough to achieve the capacity

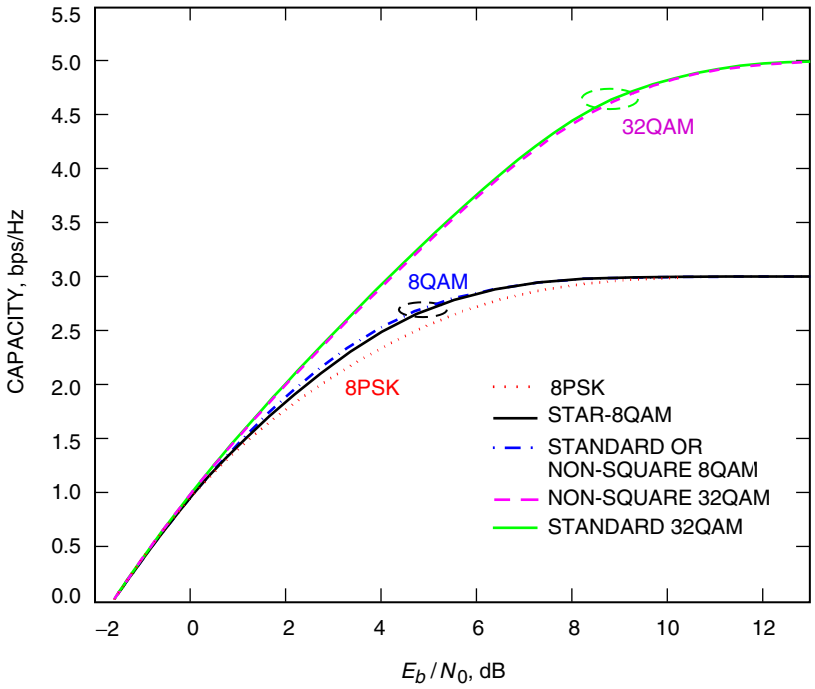

Fig. 11. Capacity comparison of the six different modulation schemes on an AWGN channel.

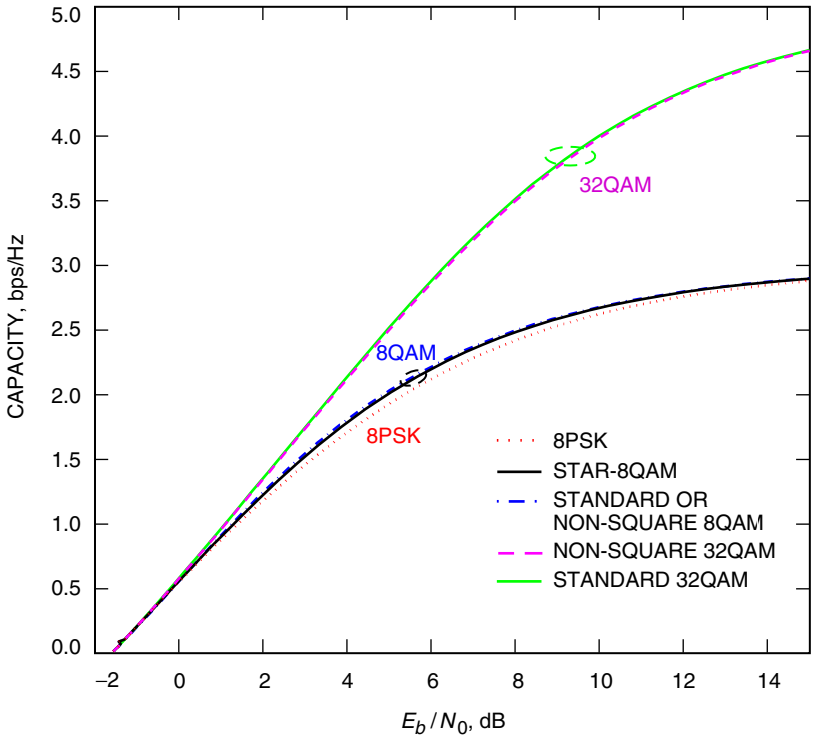

Fig. 12. Capacity comparison of the six different modulation schemes on a Rayleigh fading channel.

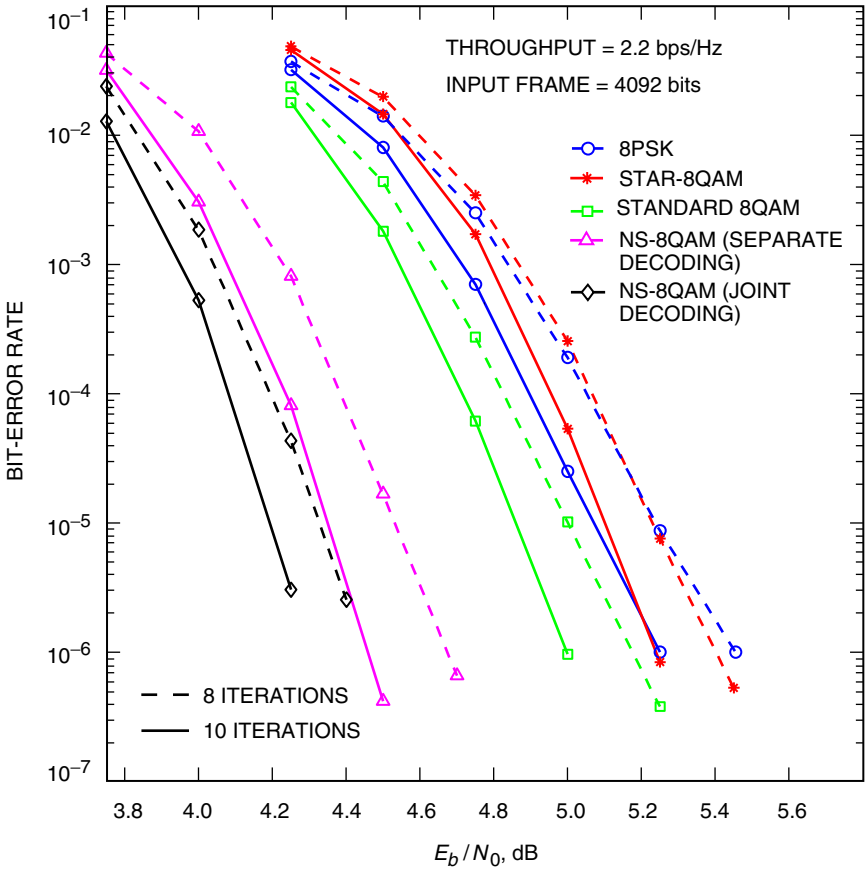

Fig. 13. BER comparison for coded NS-8QAM, standard 8QAM, star-8QAM, and 8PSK on an AWGN channel.

advantage of star-8QAM over 8PSK, although our simulation results of an alternative labeling scheme (not shown here) were even worse. Labeling (or mapping) mechanisms suitable for iterative decoding processes are discussed in [27–30].

Figure 14 compares the BER performance of coded NS-32QAM and standard 32QAM on an AWGN channel. We see that NS-32QAM, with iterative demodulation and joint decoding of the accumulator codes and the SPC code, requires an E_b/N_0 of about 7.45 dB to achieve BER $= 10^{-5}$ with 10 iterations, which is about 1.6 dB above its capacity limit. In the coded system, NS-32QAM outperforms standard 32QAM by about 0.45 dB notwithstanding standard 32QAM's slightly better capacity limit and slightly better uncoded performance. There is a loss of about 0.2 dB for NS-32QAM when the simpler, separate decoding of the accumulator codes and the SPC code is substituted for joint decoding. Compared to the improvement of coded NS-8QAM over standard 8QAM, the smaller improvement of coded NS-32QAM over standard 32QAM may be due to the larger block length of the inherent SPC code in NS-32QAM. Specifically, for NS-32QAM, one parity-check bit is added for every five output bits of the accumulators, while for NS-8QAM, one parity-check bit is added for every three output bits of the accumulators.

B. Rayleigh Fading Channel

In this subsection, we show simulation results for the six coded modulation schemes on a Rayleigh fading channel with normalized Doppler frequency $f_dT_s = 0.05$. Here f_d is the Doppler rate and $1/T_s$ is the modulation symbol rate. Figure 15 compares the BER performance of the four coded 8-ary systems on this channel. We see that, unlike the case of the AWGN channel, standard 8QAM and star-8QAM

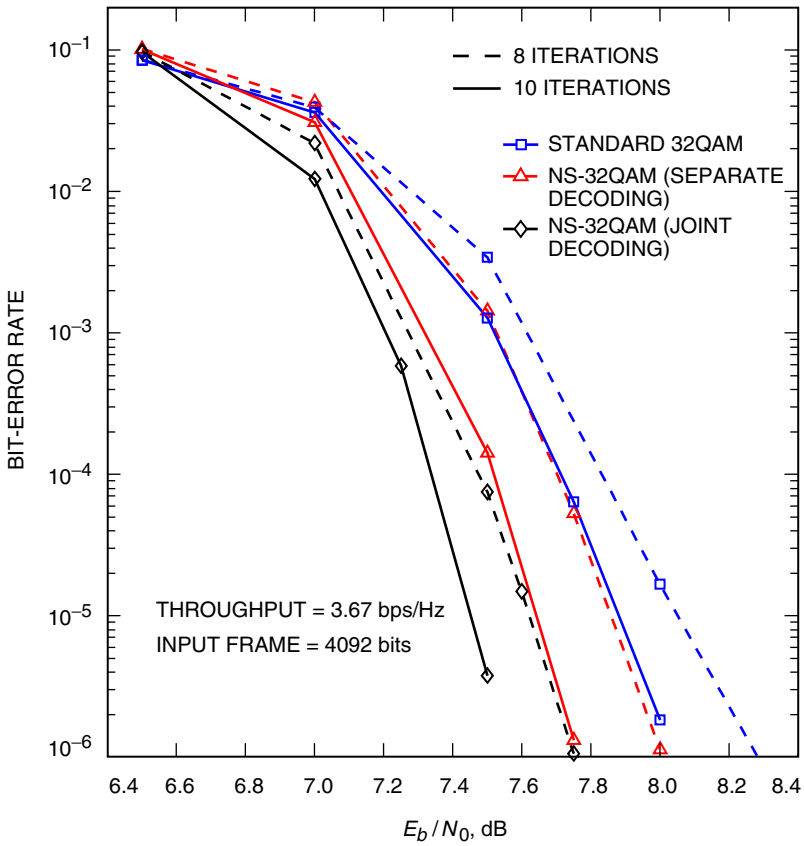

Fig. 14. BER comparison for coded NS-32QAM and standard 32QAM on an AWGN channel.

now both perform worse than 8PSK. The difference between standard 8QAM and 8PSK is negligible, but star-8QAM is about 0.1 dB worse. NS-8QAM, with iterative demodulation and joint decoding of the accumulator codes and the SPC code, outperforms standard 8QAM by about 0.57 dB at BER $= 10^{-5}$ with 10 iterations. There is a loss of about 0.12 dB when the simpler, separate decoding of the accumulator codes and the SPC code is substituted for joint decoding.

Figure 16 compares the BER performance of coded NS-32QAM and standard 32QAM on the Rayleigh channel. We see that NS-32QAM, with iterative demodulation and joint decoding of the accumulator codes and the SPC code, outperforms standard 32QAM by about 0.27 dB at BER $= 10^{-5}$ with 10 iterations. There is a loss of about 0.08 dB for NS-32QAM when the simpler, separate decoding of the accumulator codes and the SPC code is substituted for joint decoding. The improvement of coded NS-32QAM over standard 32QAM on Rayleigh fading channels is somewhat smaller than that on AWGN channels, and so is the improvement of coded NS-8QAM over the other three coded 8-ary systems. However, for both NS-8QAM and NS-32QAM, the loss associated with using the simpler, separate decoding of the accumulator codes and the SPC codes instead of the joint decoding method on Rayleigh fading channels is less than that on AWGN channels.

VI. Conclusions

We have shown that NS-2^{2n+1}-QAM ($n \geq 1$) can be decomposed into an SPC encoder and a memoryless modulator. Therefore, NS-2^{2n+1}-QAM is by itself a form of coded modulation. When NS-2^{2n+1}-QAM is concatenated with an FEC code, the overall coded system can be viewed as a serially concatenated

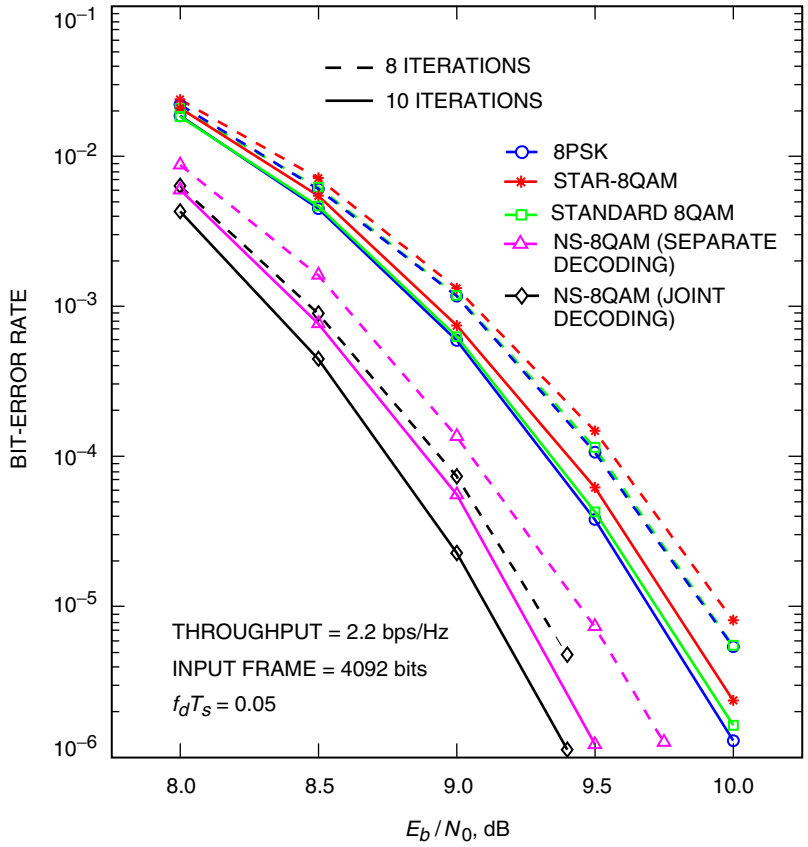

Fig. 15. BER comparison for coded NS-8QAM, standard 8QAM, star-8QAM, and 8PSK on a Rayleigh fading channel.

code followed by a memoryless modulator. We have described how to perform iterative demodulation and decoding on such a concatenated system to exploit the inherent memory of NS-2^{2n+1}-QAM and its independent I- and Q-channel mapping and demapping.

For both AWGN and Rayleigh fading channels, comparisons of the capacity and the BER/SER performances of coded and uncoded systems have been given for NS-8QAM and three other 8-ary modulations, and for NS-32QAM and standard 32QAM. We have shown that NS-8QAM has the same capacity as standard 8QAM while NS-32QAM has a slightly smaller capacity than standard 32QAM on both kinds of channels. While uncoded star-8QAM has the best asymptotic SER performance on the AWGN channel, it performs nearly 1 dB worse than uncoded NS-8QAM on the Rayleigh fading channel, and star-8QAM has smaller capacity than NS-8QAM on both types of channels. Simulation results show that coded NS-8QAM performs 0.65 dB better than standard 8QAM and 0.85 dB better than both 8PSK and star-8QAM at BER = 10^{-5} on the AWGN channel when the FEC code is a concatenation of (15,11) Hamming codes with rate-1 accumulator codes and iterative demodulation and decoding are applied. On the Rayleigh fading channel, NS-8QAM concatenated with the same FEC code performs 0.57 dB better than both standard 8QAM and 8PSK, and 0.67 dB better than star-8QAM. NS-32QAM concatenated with the same FEC code outperforms standard 32QAM by about 0.45 dB on the AWGN channel and about 0.27 dB on the Rayleigh fading channel.

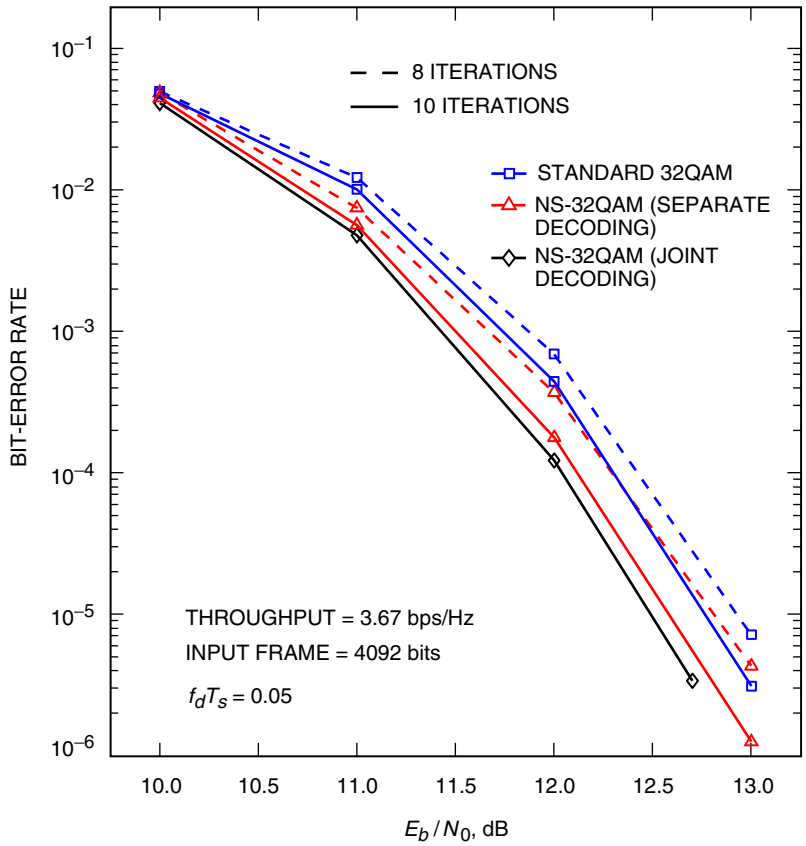

Fig. 16. BER comparison for coded NS-32QAM and standard 32QAM on a Rayleigh fading channel.

References

[1] C. Berrou, A. Glavieux, and P. Thitimajshima, "Near Shannon Limit Error-Correcting and Decoding: Turbo Codes (1)," *Proc. IEEE Int. Conf. Commun. (ICC'93)*, vol. 2, Geneva, Switzerland, pp. 23–26, May 1993.

[2] S. Benedetto, D. Divsalar, G. Montorsi, and F. Pollara, "Serial Concatenation of Interleaved Codes: Performance Analysis, Design, and Iterative Decoding," *The Telecommunications and Data Acquisition Progress Report 42-126, April–June 1996*, Jet Propulsion Laboratory, Pasadena, California, pp. 1–26, August 15, 1996.
http://tmo.jpl.nasa.gov/tmo/progress_report/42-126/126D.pdf

[3] S. Benedetto, D. Divsalar, G. Montorsi, and F. Pollara, "Serial Concatenation of Interleaved Codes: Performance Analysis, Design, and Iterative Decoding," *IEEE Trans. Inform. Theory*, vol. 44, no. 3, pp. 909–926, May 1998.

[4] C. Brutel, J. Boutros, and F. Belvèze, "Serial Encoding and Iterative Detection of Continuous Phase Modulations," *Proc. IEEE Global Commun. Conf. (GLOBECOM'99)*, vol. 5, Rio de Janeiro, Brazil, pp. 2375–2379, December 1999.

[5] K. R. Narayanan and G. L. Stüber, "Performance of Trellis-Coded CPM with Iterative Demodulation and Decoding," *IEEE Trans. Commun.*, vol. 49, no. 4, pp. 676–687, April 2001.

[6] P. Moqvist and T. M. Aulin, "Serially Concatenated Continuous Phase Modulation with Iterative Decoding," *IEEE Trans. Commun.*, vol. 49, no. 11, pp. 1901–1915, November 2001.

[7] M. R. Shane and R. D. Wesel, "Parallel Concatenated Turbo Codes for Continuous Phase Modulation," *Proc. IEEE Wireless Commun. Networking Conf. (WCNC'00)*, vol. 1, Chicago, Illinois, pp. 147–152, September 2000.

[8] M. Peleg and S. Shamai, "Iterative Decoding of Coded and Interleaved Noncoherent Multiple Symbol Detected DPSK," *Electron. Lett.*, vol. 33, no. 12, pp. 1018–1020, June 1997.

[9] P. Hoeher and J. Lodge, " 'Turbo DPSK': Iterative Differential PSK Demodulation and Channel Decoding," *IEEE Trans. Commun.*, vol. 47, no. 6, pp. 837–843, June 1999.

[10] K. R. Narayanan and G. L. Stüber, "A Serial Concatenation Approach to Iterative Demodulation and Decoding," *IEEE Trans. Commun.*, vol. 47, no. 7, pp. 956–961, July 1999.

[11] D. Divsalar and F. Pollara, "Serial and Hybrid Concatenated Codes with Applications," *Proc. Int. Symp. Turbo Codes and Applications*, Brest, France, pp. 80–87 (example 2), September 1997.

[12] P. S. K. Leung and K. Feher, "F-QPSK—A Superior Modulation Technique for Mobile and Personal Communications," *IEEE Trans. Broadcast.*, vol. 39, no. 2, pp. 288–294, June 1993.

[13] M. K. Simon and D. Divsalar, "A Reduced-Complexity, Highly Power-/Bandwidth-Efficient Coded Feher-Patented Quadrature-Phase-Shift-Keying System with Iterative Decoding," *The Telecommunications and Mission Operations Progress Report 42-145, January–March 2001*, Jet Propulsion Laboratory, Pasadena, California, pp. 1–17, May 15, 2001.
http://tmo.jpl.nasa.gov/tmo/progress_report/42-145/145A.pdf

[14] M. K. Simon and D. Divsalar, "Further Results on a Reduced-Complexity, Highly Power-/Bandwidth-Efficient Coded Feher-Patented Quadrature-Phase-Shift-Keying System with Iterative Decoding," *The Interplanetary Network Progress Report 42-146, April–June 2001*, Jet Propulsion Laboratory, Pasadena, California, pp. 1–7, August 15, 2001.
http://tmo.jpl.nasa.gov/tmo/progress_report/42-146/146I.pdf

[15] M. K. Simon and D. Divsalar, "A Reduced Complexity Highly Power/Bandwidth Efficient Coded FQPSK System with Iterative Decoding," *Proc. IEEE Int. Conf. Commun. (ICC'01)*, vol. 7, Helsinki, Finland, pp. 2204–2210, June 2001.

[16] D. Divsalar and S. Dolinar, "Performance of a High-Speed Concatenated Coded Modulation Scheme over Fading Channels," *Proc. IEEE Military Commun. Conf. (Milcom'03)*, Boston, Massachusetts, October 2003.

[17] J. A. Torres, "Method for Using Non-Squared QAM Constellations," Forum Contribution, IEEE 802.16 Broadband Wireless Access Working Group, May 23, 2002.
http://www.ieee802.org/16/tga/contrib/C80216a-02_66.pdf

[18] S. Benedetto, D. Divsalar, G. Montorsi, and F. Pollara, "A Soft-Input Soft-Output Maximum A Posteriori (MAP) Module to Decode Parallel and Serial Concatenated Codes," *The Telecommunications and Data Acquisition Progress Report 42-127, July–September 1996*, Jet Propulsion Laboratory, Pasadena, California, pp. 1–20, November 15, 1996.
http://tmo.jpl.nasa.gov/tmo/progress_report/42-127/127H.pdf

[19] S. Benedetto, D. Divsalar, G. Montorsi, and F. Pollara, "A Soft-Input Soft-Output APP Module for Iterative Decoding of Concatenated Codes," *IEEE Commun. Lett.*, vol. 1, no. 1, pp. 22–24, January 1997.

[20] L. R. Bahl, J. Cocke, F. Jelinek, and J. Raviv, "Optimal Decoding of Linear Codes for Minimizing Symbol Error Rate," *IEEE Trans. Inform. Theory*, vol. IT-20, no. 2, pp. 284–287, March 1974.

[21] A. Ambroze, G. Wade, and M. Tomlinson, "Iterative MAP Decoding for Serial Concatenated Convolutional Codes," *IEE Proc.-Commun.*, vol. 145, no. 2, pp. 53–59, April 1998.

[22] R. D. Wesel, X. Liu, J. M. Cioffi, and C. Komninakis, "Constellation Labeling for Linear Encoders," *IEEE Trans. Inform. Theory*, vol. 47, no. 6, pp. 2417–2431, September 2001.

[23] J. G. Proakis, *Digital Communications*, 2nd. ed., New York: McGraw-Hill, p. 281, 1989.

[24] S. Benedetto and E. Biglieri, *Principles of Digital Transmission: With Wireless Applications*, New York: Kluwer Academic/Plenum Press, p. 196, 1999.

[25] M. K. Simon and M.-S. Alouini, *Digital Communication Over Fading Channels*, New York: John Wiley & Sons, Inc., p. 219, 2000.

[26] R. E. Blahut, *Principles and Practice of Information Theory*, Reading, Massachusetts: Addison-Wesley, p. 275, 1990.

[27] A. Gorokhov and M. van Dijk, "Optimised Labeling Maps for Bit-Interleaved Transmission with Turbo Demodulation," *Proc. IEEE Veh. Tech. Conf. (VTC'01)*, vol. 2, Rhodes, Greece, pp. 1459–1463, May 2001.

[28] J. Tan and G. Stüber, "Analysis and Design of Interleaver Mappings for Iteratively Decoded BICM," Proc. IEEE Int. Conf. Commun. (ICC'02), vol. 3, pp. 1403–1407, 2002.

[29] S. ten Brink, J. Speidel, and R.-H. Yan, "Iterative Demapping for QPSK Modulation," Electron. Lett., vol. 34, no. 15, pp. 1459–1460, July 1998.

[30] S. ten Brink, J. Speidel, and R.-H. Yan, "Iterative Demapping and Decoding for Multilevel Modulation," *Proc. IEEE Global Commun. Conf. (GLOBECOM'98)*, vol. 1, Sydney, Australia, pp. 579–584, November 1998.